Polymeric single Li^+-ion conductors: preparation and characterisation

Thesis report for Degree of Master of Science in Chemical Engineering

Author: Hannes Nederstedt

Division of Polymer and Material Chemistry, Faculty of Engineering, Lund University, Sweden

June 2016

Supervisor:
Dr Zhecheng Shao, Lund University, Sweden

Examiner:
Professor Patric Jannasch, Lund University, Sweden

Abstract

Lithium-ion batteries are a common type of light-weight, rechargeable batteries. There are safety concerns because these batteries typically use an organic solvent electrolyte which presents fire hazards. By using dry polymer electrolytes, the fire hazards can be eliminated. The single-ion conductor is a type of polymer electrolyte in which the ion-containing group has been covalently bonded with the polymer structure, thereby immobilising the anion. This eliminates problems present in common liquid electrolytes, such as dendritic growth in the battery that can lead to short circuiting.

The purpose of this Master thesis was to synthesise and characterise single-ion conductors. The polymers were random copolymers with a poly(ethylene oxide) backbone. The ion-containing repeating units contained a side chain with one quaternary ammonium cation and two sulfonate anions. The non-ionic repeating units carried a triethylene glycol monomethyl ether side chain. Copolymerisation by anionic and cationic ring-opening mechanism failed. Instead poly(epichlorohydrin) was synthesised using an anionic ring-opening mechanism followed by several post-polymer reactions to yield the target polymers. These polymers did not form a melt at sufficiently low temperatures (below 140 °C) in order to make samples for conductivity measurements. Instead blends between homopolymer only containing ionic repeating units and poly(ethylene glycol-ran-propylene glycol) were made and the conductivity of these blends were measured. The highest measured conductivity was $3.3 \cdot 10^{-6}$ S/cm at 90 °C for a blend with an EO/Li ratio of 8. This conductivity, while similar to other single-ion conductors, is too low for the blends to be used for battery applications.

Suggestion for future work include the preparation of polymers with sulfonate groups that are more rigidly bonded to the polymer to inhibit the tight coordination of lithium ions by the polymer, thereby improving the conductivity. Copolymers with large amount of non-ionic repeating units should be synthesised to further decrease their glass transition temperature and make measurements by impedance spectroscopy possible.

Acknowledgements

This Master thesis has been performed at the Division of Polymer & Materials Chemistry at Lund University during the spring of 2015 under the supervision of Zhecheng Shao.

I would like to thank Zhecheng Shao for his extensive help and support, Patric Jannasch for giving me the opportunity of working on this project and Thanh Huong Phan, Joel Olsson, Hai-Son Dang and Matilda Larsson for their help when Shao was unavailable.

Nomenclature

$Al(i\text{-}Bu)_3$	Triisobutylaluminium
c_k	Concentration of ion k (mol litre^{-1})
C. B.	Conduction band
D	Salt diffusion coefficient (cm^2 s^{-1})
D_k	Diffusion coefficient of ion k (cm^2 s^{-1})
DMC	Dimethyl carbonate
DSC	Differential scanning calorimetry
EC	Ethylene carbonate
ECH	Epichlorohydrin
EO_3Gly	Triethylene glycol monomethyl ether
EO_3Ox	2-(2,5,8,11-tetraoxadodec1-yl)-oxirane
F	Faradays constant (96 485 C mol^{-1})
HOMO	Highest occupied molecular orbital
i	Current density (A cm^{-1})
ImTFSI	Imidazolium bistrifluoromethylsulfonimide
j	Imaginary unit $j^2 = -1$
LIB	Lithium-ion battery
Li^+	Lithium ion
$LiPF_6$	Lithium hexafluorophosphate
LiTFSI	Lithium bis-trifluoromethylsulfonimide
LUMO	Lowest unoccupied molecular orbital
M_n	Number average molecular weight
M_w	Weight average molecular weight
NMR	Nuclear magnetic resonance
$NOct_4Br$	Tetraoctylammonium bromide
PEO	Poly(ethylene oxide)
PVBnHexIM	Poly(4-vinylbenzylhexylImTFSI)
SEC	Size exclusion chromatography
t^+	Cation transference number
Tg	Glass transition temperature
TGA	Thermogravimetric analysis
u_k	Mobility of ion k (mol m N^{-1} s^{-1})
v	Electrolyte bulk velocity (m s^{-1})
V. B.	Valence band
μ_A	Electrochemical potential at the anode (V)
μ_C	Electrochemical potential at the cathode (V)
σ	Ionic conductivity (S cm^{-1})
$\nabla\phi$	Electrochemical potential gradient (V cm^{-1})

Table of content

1. Introduction

In the modern world there is an increasing demand for smaller and lighter batteries with higher energy storage capacity and shorter charging times, both to satisfy the requirements of consumer products such as mobile phones and as power sources in electrical vehicles. Lithium is a light-weight alkali metal which is readily oxidised and is hence interesting for battery applications. The lithium-ion batteries (LIBs) are a type of rechargeable, lithium based battery with high energy density, that was first made commercially available by Sony in 1991 [1]. LIBs typically use lithium salts dissolved in an organic solvent as electrolyte which causes safety concerns in that a catastrophic failure of a LIB often begin with ignition of the electrolyte resulting in fire and explosion hazards [2]. By using dry polymer electrolytes, the presence of organic solvent and the fire hazard of LIBs can be eliminated. A large portion of the researched polymers in the field of dry polymer electrolytes are based on poly(ethylene oxide) (PEO) after it was discovered, in 1973 by P.V. Wright, that PEO can dissolve alkali salts [3].

The purpose of this thesis work is to synthesise and characterise a series of copolymers for application as polymer electrolytes in LIBs. The polymer backbone is similar to PEO. These copolymers carry ionic side chains to introduce the charge carriers and non-ionic side chains consisting of triethylene glycol monomethyl ether for the dissolution and conduction of ions. After synthesis the polymer will be characterised by differential scanning calorimetry (DSC), thermogravimetric analysis (TGA) and alternating current impedance spectroscopy.

2. Theory

2.1. Batteries and electrochemical cells

A battery is made of one or more interconnected electrochemical cells which consist of two electrodes, an anode and a cathode, separated by an electrolyte and connected through an external circuit. Figure 1 illustrates the first commercial LIB, where lithium intercalated in a graphite matrix is used as anode and cobalt oxide as cathode. The cell reactions are illustrated in equations 1-3 below. During the discharge of the LIB lithium at the cathode oxidises, lithium cations (Li^+) travel through the electrolyte and electrons travel through an external circuit to the cathode where they form an intercalation compound with the cobalt oxide [4]. During the charge of the LIB the opposite process occurs. No lithium metal is ever present which eliminates the hazards present in batteries using an electrode made of lithium [4]. The electrolyte conducts ions between the electrodes to maintain the process while keeping the electrodes separated and inhibiting transfer of electrons through the electrolyte to avoid short circuiting and enable the use of an external circuit [5].

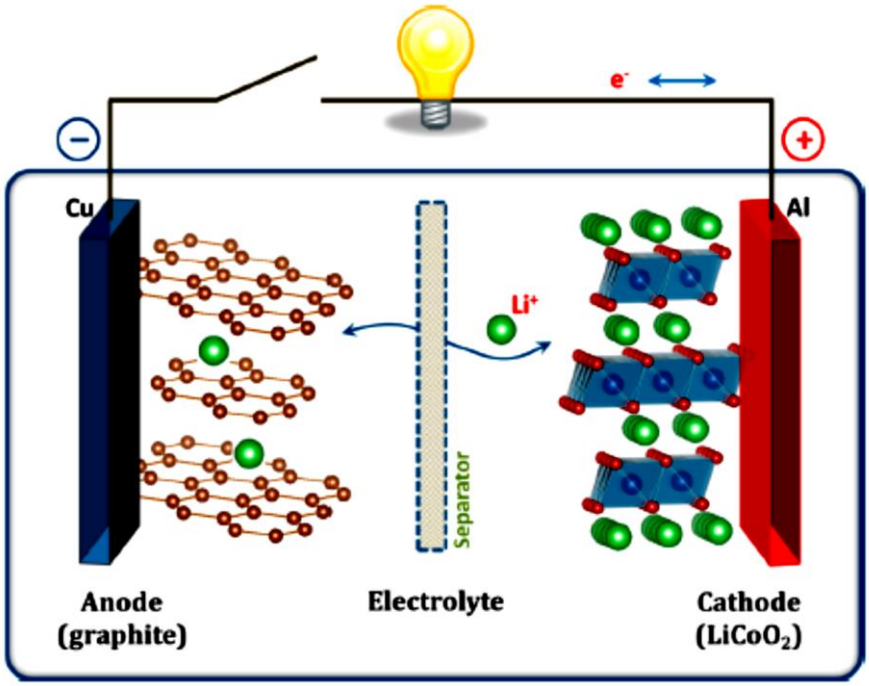

Figure 1. Illustration of the first commercial lithium-ion cell [5]

Anode: $$Li_xC_6(s) \leftrightharpoons x\,Li^+ + 6\,C + x\,e^-$$ 1.

Cathode: $$x\,Li^+ + CoO_2(s) + x\,e^- \rightleftharpoons Li_xCoO_2(s)$$ 2.

Overall cell: $$Li_xC_6(s) + CoO_2(s) \rightleftharpoons 6\,C + Li_xCoO_2(s)$$ 3.

2.2. Ion transport terms

The transport of ionic species in the electrolyte is governed by gradients in the electrochemical potential, $\nabla\phi$. For a dilute mixture of a univalent salt where all salt is completely dissociated in the electrolyte the current density, i (A cm^{-1}), can be described with equation 4 below [2].

$$i = -F^2\nabla\phi \sum_{k=+,-} u_k c_k - F\sum_{k=+,-} D_k \nabla c_k + Fv \sum_{k=+,-} c_k \quad 4.$$

Where u_k is the mobility of ion k (mol m N^{-1} s^{-1}), D_k is the diffusion coefficient (cm^2 s^{-1}), c_k is ion concentration (mol dm^{-3}), v is the bulk velocity of the electrolyte (m s^{-1}) and F is Faradays constant (96 485 C mol^{-1}). The first term to the right hand side is the current due to transport of ions in a potential gradient (voltage) and is the main cause of current in an electrochemical cell. The second is due to the diffusion of ions in a concentration gradient and the third accounts for convection of ion and is zero due to electroneutrality ($c_+ + c_- = 0$). Of the four transport coefficients (u_+, u_-, D_+ and D_-) only three are independent and the coefficients are often rewritten as the three transport properties, ionic conductivity, salt diffusion coefficient, and cation transference number [2]. These transport properties have been determined in a large number of classical electrolytes, however electrochemical characterisation of polymer electrolytes is often limited to measurements of the ionic conductivity [2]. In an electrolyte without concentration gradients the ionic conductivity, σ, is given by equation 5 below and is measured using alternating current impedance spectroscopy [2].

$$\sigma = -\frac{i}{\nabla\phi} = -F^2(u_+c_+ + u_-c_-) \quad 5.$$

The salt diffusion coefficient, D, is defined as the mobility-weighted mean diffusion coefficient of the ions presented in equation 6 below [2]. D is measured by using a symmetric cell with reversible electrodes that is polarised and relaxation of the polarisation, after the polarising field is turned off, is measured [2]. After a long time, the cell is only slightly perturbed and the change in the measured potential is only due to change in concentration gradient, from this change in potential the diffusion coefficient is obtained.

$$D = \frac{u_+D_+ + u_-D_-}{u_+ + u_-} \quad 6.$$

The transference number t^k is the fraction of charge carried by ion k in the absence of a concentration gradient. The cation transference number, t^+, is given by equation 7 below. Transference number measurement involves polarising a cell with reversible electrodes, while limiting the concentration gradient to the regions near the electrodes, and determining the salt concentration profile [2].

$$t^+ = 1 - t^- = \frac{u_+}{u_+ + u_-} \quad 7.$$

A t^+ of unity signifies that the entire current is carried by the cations. When t^+ is less than one, mobile anions in the electrolyte of an LIB will be transported by the potential gradient to the anode, where they will accumulate due to not reacting at the anode which leads to concentration gradients of anions and cations in the electrolyte. The concentration gradient leads to electropolarisation which lowers the overall cell performance, voltage losses and dendritic growth. Dendritic growth is when lithium deposits and creates metal bridges between the electrodes which leads to internal short circuiting and may lead to ignition and explosion of the battery [5].

2.3. Types of electrolytes

Electrolytes need to meet the following requirements [6]

- Have a high conductivity ($\sigma > 10^{-4}$ S/cm for polymer electrolytes) at the operating temperature
- Keep the electrodes separated
- Appreciable lithium transference number
- Be compatible with the electrodes
- Be thermally and electrochemically stable

High conductivity is necessary for sufficient transport of ions through the electrolyte. In the case of solid electrolytes, a sufficiently high mechanical strength of the electrolyte is necessary to keep the electrodes separated. High mechanical strength could permit the use of a thinner electrolyte film decreasing the overall resistance of the electrolyte and increasing the weight percentage of energy producing electrodes, thereby increasing the energy density of the electrochemical cell. The transference number should be high to allow the lithium ions to be the primary charge carriers and minimise concentration gradients. The electrolyte needs to be compatible and have complete contact with the electrodes.

The electrolyte needs to be thermally stable at the operating temperature and electrochemically stable at the electric potentials present in the battery in order to not decompose and lose its properties. Figure 2 illustrates the relative energies of the components in an electrochemical cell, if the LUMO (lowest unoccupied molecular orbital) for a liquid electrolyte or the bottom of the conduction band (C.B.) in a solid electrolyte is lower in energy than the potential at the anode (μ_A) the electrolyte will be reduced at the anode. Similarly, if the HOMO (highest occupied molecular orbital) for a liquid electrolyte or the top of the valence band (V.B.) in a solid electrolyte is higher in energy than the potential at the cathode (μ_C) the electrolyte will be oxidised at the cathode. The electrolyte is electrochemically stable within a potential interval in which it is neither oxidised nor reduced by the electrodes [5]. Electrolytes are often unstable at the operating potentials, instead a passivating layer is formed at the electrode-electrolyte interface which protects the bulk electrolyte [2]. The stability of this passivating layer often limits the lifetime of modern LIBs.

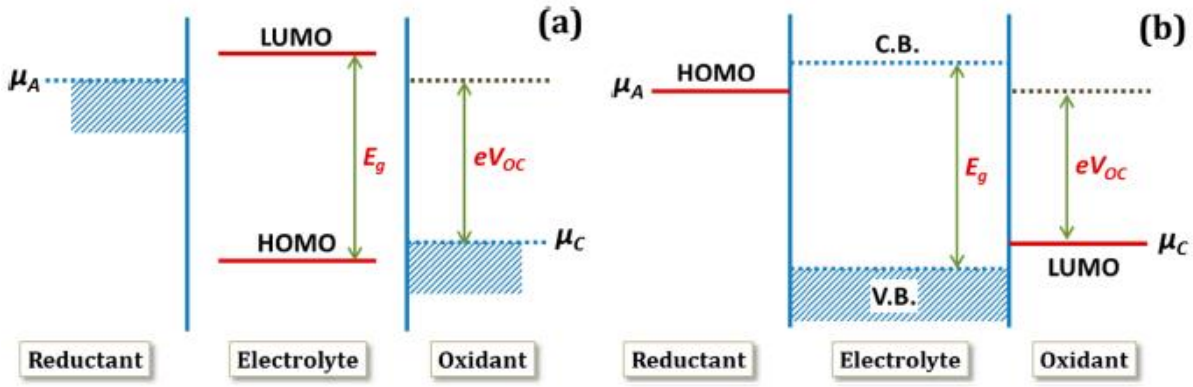

Figure 2. Relative energies of the anode (Reductant), cathode (Oxidant) and electrolyte in an electrochemical cell using a: liquid and b: solid electrolyte [5]

Hallinan and Balsara define four types of homogenous electrolytes that can be used in LIBs, where the electrolyte is a single phase and macroscopically homogenous [2].

- **Type I: classical electrolyte**. A mixture of salts in a low molecular weight solvent.
- **Type II: gel electrolyte.** A polymer network swollen with a classical electrolyte. The polymer does not participate in ion solvation.
- **Type III: dry polymer electrolyte.** A mixture of salts in a high molecular weight polymer. The polymer participates in ion solvation
- **Type IV: dry single-ion conductor.** One type of ion (anion or cation) is covalently bound to the polymer backbone. The polymer participates in ion solvation.

Table 1. Examples of electrolytes and their properties [2]

Type	Electrolyte	Concentration mol litre^{-1}	Temperature (°C)	σ (S cm^{-1})	D (cm^2 s^{-1})	t^+	Voltage stability (V)
I	Organic liquid ($LiPF_6$ in EC/DMC)	1	25	1×10^{-2}	3×10^{-6}	0.38	1.3-4.6
I	Ionic liquid (ImTFSI)	4.0	80	1×10^{-2}	7×10^{-7}	0.46	-
II	Organic gel ($LiClO_4$ in EC/PC + PAN)	1.5	25	2×10^{-3}	-	0.5	1.0-4.6
III	Polymer (LiTFSI in PEO)	1.5	85	1×10^{-3}	1×10^{-7}	0.41	0.5-3.8
IV	Poly(ionic liquid) (PVBNHexIMTFSI)	2.0	90	4×10^{-5}	-	0	-
IV	Cross-linked polymer (PAE-XE)	0.9	85	5×10^{-6}	-	1	-

A few examples of electrolytes are shown in Table 1. Commercial LIBs typically use the classical electrolyte with a lithium salt, such as $LiPF_6$ (lithium hexafluorophosphate), dissolved in an organic solvent, such as a mixture of dimethyl carbonate (DMC) and ethylene carbonate (EC). The classical electrolytes have high ionic conductivity and are able to form a stable contact with the electrodes but the presence of organic solvent presents a fire and explosion hazard.

The second example of a type I electrolyte ImTFSI (imidazolium bistrifluoromethylsulfonimide) is a ionic liquid, a salt with a melting point below 100 °C [7]. Due to the lack of solvent the moles of charge carrier per litre is higher than for the electrolytes using organic solvent. When the temperature is above the melting point of the ionic liquid, the conductivity and transference number is similar to electrolytes using organic solvent. The flammability of ionic liquids is low and the electrochemical stability is high [2].

The other types all involve the use of polymers. The type II uses a classical electrolyte as the conductive part and a polymer network to provide mechanical properties resulting in transport properties to the type I with a lower conductivity due to the polymer chains in the gel impeding ion motion. The example in Table 1 is a poly(acrylonitrile) (PAN) gelled with EC and propylene carbonate (PC) and lithium perchlorate ($LiClO_4$) dissolved in the solvent.

In type III electrolytes a lithium salt, often with a bulky delocalized anion such as LiTFSI (lithium bis-trifluoromethylsulfonimide), is dissolved in a polymer such as poly(ethylene oxide) (PEO). Many of the type III and IV electrolytes incorporates ethylene oxide in some way into their structures. The conductivity is lower compared to type I and II but the fire hazard is eliminated due to the absence of organic solvents.

Type I, II and III electrolyte have a transference number well below unity, leading to concentration gradients of ions in these electrolyte [6]. In single-ion conductors one of the ionic species is covalently bonded to the polymer backbone, greatly reducing its mobility. By bonding the anion, the lithium transference number can be close to unity. This reduces the concentration gradients and the issues caused by them. The ionic conductivity of single-ion conductors is typically lower than the conductivity of type III, however a single-ion conductor with lithium transference number of unity is comparable to an electrolyte with transport of both ionic species even with a tenfold reduction of the ionic conductivity [8]. In single-ion conductors there is still some finite mobility of the polymer chains resulting in a transference number that is typically less than unity. The cations and anions are not separated and distributed uniformly, due to one type of ion being immobilised by bonding it to the polymer, which is why type IV is termed single-ion conductor and not single-ion electrolyte.

The first example of a type IV electrolyte is a poly(ionic liquid) with an Im^+ cation bound to the polymer backbone and a mobile $TFSI^-$ anion. Poly(ionic liquid) are polymers in which ionic liquids have been incorporated into the polymer structure and have some properties similar to ionic liquids. Poly(ionic liquids) typically have a reduced conductivity compared to ionic liquids however the mechanical properties are improved. In PVBnHexImTFSI (poly(4-vinylbenzylhexylImTFSI)) the cation is immobilised and the anion is mobile which results in a t^+ equal to zero.

The second example of a type IV electrolyte is an electrolyte in which a bis(allylmalonato)borate anion has been covalently bound to a cross-linked polymer (polyacrylate with eight ethylene oxide units in the cross-links and five in the side chains) and lithium cations are mobile. This electrolyte resembles an electrolyte with a PEO matrix doped with a lithium salt in which the anion has been immobilised which results in a t^+ equal to one.

2.4. Mechanism of ion conduction in PEO

Ion conduction in amorphous PEO above the glass transition temperature (T_g) occurs by two mechanisms [2]. The lowest free-energy configuration of lithium ions dissolved in PEO consist of the ion coordinated with six ether oxygens, as shown in Figure 3a below. In the first mechanism of conduction, shown in Figure 3b and Figure 3c, segmental motion of polymer chains will break the lithium-oxygen causing the diffusion of lithium ions toward sites of lower free energy where a new coordination complex is formed. This mechanism is called fluctuation-driven diffusion and is affected by the T_g of the polymer electrolyte where a lower T_g results in more motion and hence higher conduction. Since the T_g of a polymer increases with molecular weight toward a plateau value, fluctuation-driven diffusion will decrease with and eventually become independent of the molecular weight.

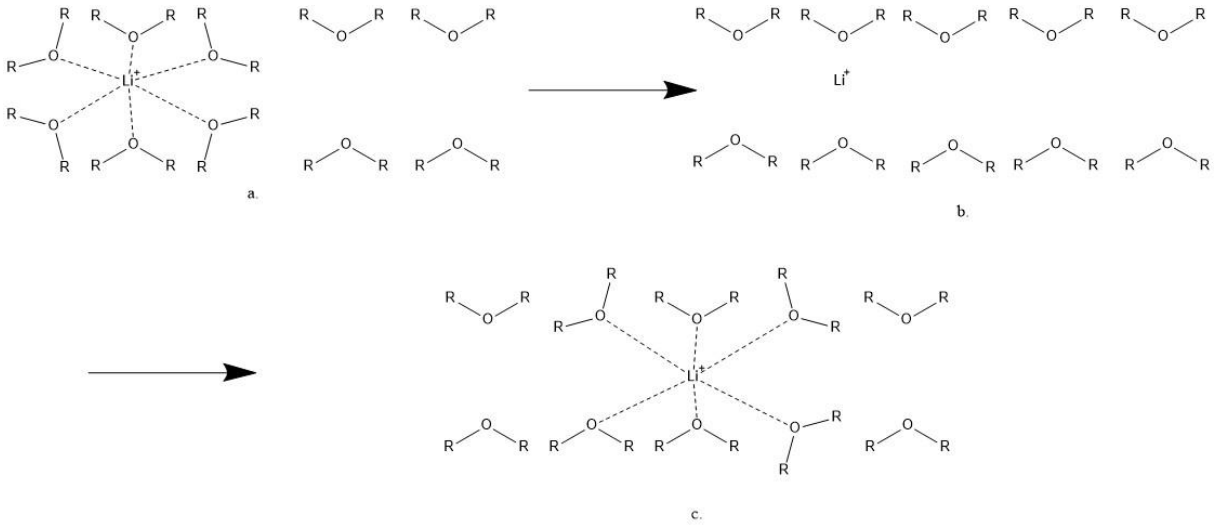

Figure 3. Illustration of fluctuation-driven diffusion, R = chain of PEO, **a.** lithium ion coordinated by six ether oxygens, **b.** the coordination is broken, **c.** lithium diffuses toward a site of lower free energy (along the potential gradient) where a new coordination complex is formed.

The second mechanism of conduction is vehicular diffusion, which involves diffusion of the entire coordination complex [2]. Vehicular diffusion is only applicable in low molecular weight polymers due to the polymer-ion complex becoming entangled in the polymer matrix hindering diffusion hence fluctuation-driven diffusion dominates at higher molecular weights. The mechanism of conduction in low molecular weight solvents is similar to the mechanisms described above with vehicular diffusion as the dominating type. A few reports have indicated that crystalline PEO can have a higher ionic conductivity than amorphous PEO but overall it is considered that the amorphous regions conduct ion and crystallisation is detrimental to ion transport [1], making it necessary to use PEO above its melting temperature (67 °C). Generally, methods to increase the amount of amorphous PEO such as addition of plasticizer has been used to improve the ionic conductivity. Increasing the salt concentration in the polymer increases the amount of charge carrier but typically increases T_g which decreases conductivity for each charge carrier. With respect to ionic conductivity, there is an optimal salt concentration that the PEO can be doped with often expressed as the ratio between ethylene oxide repeating units and Li^+ ions (EO/Li ratio).

2.5. Anionic ring-opening polymerisation of epichlorohydrin

Polymerisation of epichlorohydrin (ECH) with conventional anionic initiator is not possible due to the reaction between the chloromethyl group and the highly nucleophilic propagating species [9]. ECH has previously been polymerised using a tetraoctylammonium bromide ($NOct_4Br$) - triisobutylaluminium ($Al(i\text{-}Bu)_3$) system [9], as shown in Figure 4 below. $NOct_4Br$ and $Al(i\text{-}Bu)_3$ form an initiating complex and $Al(i\text{-}Bu)_3$ activates monomer for propagation, during propagation the aluminate complex attacks monomer activated by $Al(i\text{-}Bu)_3$. No polymerisation occurs at a [$Al(i\text{-}Bu)_3$]/[$NOct_4Br$] ratio equal to one since there is no aluminium available for monomer activation. With this catalytic system polyepichlorohydrin (PECH) with high and narrowly distributed molecular weight can be synthesised [9].

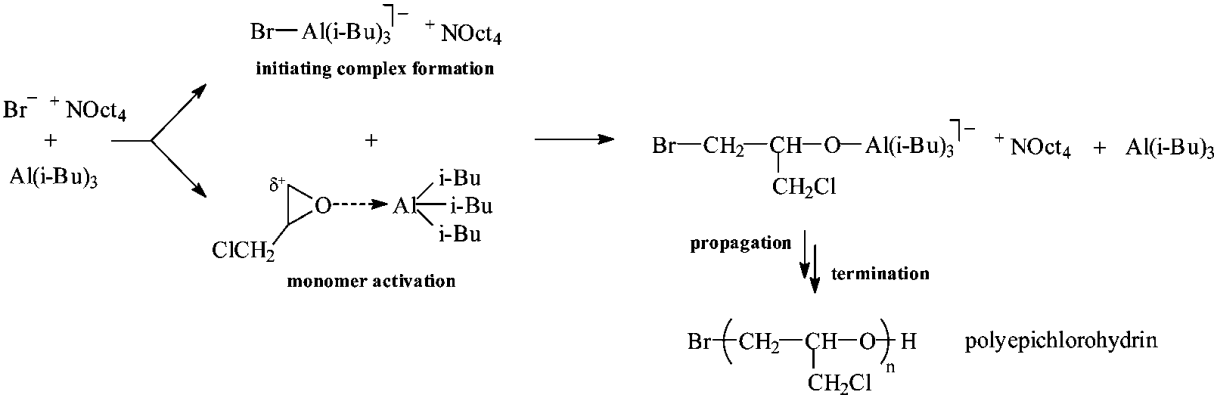

Figure 4. Polymerisation of ECH using $NOct_4Br/Al(i\text{-}Bu)_3$ system [9]

2.6. Target polymer

The target polymer is shown in Figure 5 below. This polymer is a random copolymer with one non-ionic repeating unit and one repeating unit that has two anionic charges and one cationic charge giving it a net negative charge. The cation transference number will be close to unity due to the net negative charge of the ionic repeating units. The ratio between ionic and non-ionic repeating units is varied in order to find an optimal EO/Li ratio.

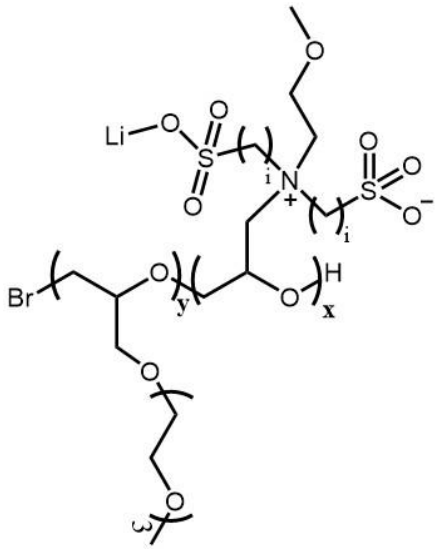

Figure 5. Target polymer, x and y denotes molar fractions of the repeating units, i = 2 or 4

2.7. Nuclear magnetic resonance (NMR) spectroscopy

When placed in a magnetic field some isotopes of atoms such as ^{1}H (hydrogen-1) and ^{13}C (carbon-13) absorb electromagnetic radiation at a characteristic frequency. In nuclear magnetic resonance (NMR) spectroscopy a sample is subjected to a magnetic field and the absorption at different frequencies is measured. An NMR spectrum will show peaks at frequencies where the radiation is absorbed. The ^{1}H in a sample can be studied with NMR spectroscopy, the exact frequency and shape of the peaks is dependent of the chemical environment in the molecule, and the peaks can be used to identify which molecules are present in the sample. In samples containing low weight molecules there are many identical ^{1}H and the difference in the environment of different ^{1}H is large which often results in sharp distinct peaks present in an NMR spectrum. In the case of NMR spectroscopy of polymers there are many ^{1}H with similar chemical environment, ^{1}H on a repeating unit have similar absorption frequency but slightly different depending on which repeating unit it is in the polymer structure, but few with exactly the same environment. This causes polymers to have peaks in a NMR spectrum that are broadened compared to its monomers.

2.8. Size exclusion chromatography (SEC)

Size exclusion chromatography (SEC) is a chromatography technique used to determine a polymer molecular weight distribution. The stationary phase is a mechanically stable, crosslinked gel with a distribution of different pore sizes [10]. Separation of the polymers by their molecular weight takes place due to the fact that polymers with high molecular weight are excluded from the smaller pore sizes and have a lower elution volume than the low weight polymers. Due to axial dispersion controlled by molecular diffusion the elution volume of a particular molar weight is slightly broadened causing some overlap in when polymers with different molecular weights overlap and hence introducing some errors in the measurement [10]. The polymer concentration in the eluate is measured using for example refractive index, UV or IR detectors. By using a standard sample of a polymer with known molecular weight for calibration the elution volume can be related to the molecular weight. From the molecular weight distribution different averages of the molecular weight, such as the number average M_n and weight average M_w, can be calculated.

$$M_n = \frac{\sum_i M_i \cdot N_i}{\sum_i N_i} \quad (9.)$$

$$M_w = \frac{\sum_i M_i^2 \cdot N_i}{\sum_i M_i \cdot N_i} \quad (10.)$$

$$PDI = \frac{M_w}{M_n} \quad (11.)$$

Where N_i is the number of moles of polymer with the molecular weight M_i and the polydispersity index (*PDI*) is a measurement of how wide the molecular weight distribution is.

2.9. Thermal analysis

Thermogravimetric analysis (TGA) is a thermal analysis method in which a sample is heated under a flow of a gas and the mass of the sample at different temperatures is measured. Loss of mass can be attributed to physical phenomena such as vaporisation and sublimation, or chemical phenomena such as decomposition of the sample. Mass gain can be attributed to chemical reaction with the atmosphere such as oxidation. TGA can be performed using different flows of gases over the sample, with an oxygen flow the oxidation of the sample can be studied and with a nitrogen flow phenomena such as decomposition can be studied.

Differential scanning calorimetry (DSC) involves the heating of a sample in a closed pan. The sample is put in one heating chamber and an empty reference pan is put in another heating chamber. The temperature in both chambers is changed and the difference in heating power required to keep both heating chambers at the same temperature is measured at different temperatures [11]. The result of the measurement is commonly presented in a DSC curve with the differential heat flow as a function of the temperature in the chambers. Second-order transition in which the heat capacity of the sample suddenly changes is presented in the curve as a sudden change in slope and is observed at the glass transition temperature of the polymer sample [11]. Exo- and endothermic processes such as melting and crystallisation are presented as peaks in the curve [11].

2.10. Impedance spectroscopy

Electrical impedance (*Z*) is the opposition to a current when a voltage is applied on a circuit. For direct current (DC) the impedance is equivalent to the resistance of the circuit. For alternating current (AC), the impedance is the complex ratio of the voltage to the current and can be presented with a real and an imaginary part, as shown in equation 12 below (where $j^2 = -1$, *j* is used in this thesis as to not confuse it with the current density *i*) [12]. The real part, *Z'*, of the impedance is the resistance and the imaginary part, *Z''*, called reactance takes into account voltages in the circuit caused by the magnetic fields of currents (inductance) and electrostatic storage of charge induced by voltages in the circuit(capacitance) [12]. Both properties are dependent of the frequency, f, of the AC which is usually rewritten as the angular frequency, $\omega = 2\pi f$. Impedance can be calculated from equation 13 by applying a voltage with a known magnitude (*U*), which is usually small ~10 mV [2], and angular frequency to the sample electrolyte while measuring the magnitude (*I*) and phase shift (φ) of the current with respect to the applied voltage. The conductivity, σ, is calculated as the inverse of the magnitude of the impedance. The measurements are performed at different frequencies of the AC and at different temperatures.

$$Z(\omega) = Z'(\omega) + j \cdot Z''(\omega) \quad (12)$$

$$Z(\omega) = \frac{U(\omega)}{I(\omega)} \cdot \exp\big(j \cdot \phi(\omega)\big) \quad (13)$$

3. Experimental

3.1. Chemicals

(±) Epichlorohydrin (ECH, Fluka Analytical, > 99 %)[1], triethylene glycol monomethyl ether (EO_3Gly, Fluka Chemica, > 97 %) and 1,4-butanediol (Riedel de Haen) were distilled before use. Tetraoctylammonium bromide ($NOct_4Br$, Aldrich, 98 %) was dried under vacuum at 50 °C dissolved in anhydrous toluene to give 50 mg/ml. 2-methoxyethylamine (TCI, > 98 %) was degassed before use.

Dichloromethane (Honeywell, Reagent grade), triisobutylaluminium 1.1 M solution in toluene ($Al(i\text{-}Bu)_3$, Acros Organics), toluene (Sigma-Aldrich, Anhydrous, 99.8 %), boron trifluoride diethyletherate (Sigma-Aldrich, purified by redistillation > 46.5 % BF_3 basis), chloroform (Honeywell, Reagent grade), hexane (Sharlau, > 99 %), N,N-dimethylformamide (DMF, Honeywell, Reagent grade), 1-methyl-2-pyrrolidinone (NMP, Acros Organics, 99 %), sodium 2-bromoethanesulfonate (Sigma-Aldrich, 98 %), 1,4-butanesultone (Sigma-Aldrich, > 99 %) and poly(ethylene glycol-ran-propylene glycol) (P[EO-r-PO], Sigma-Aldrich, M_n ~ 12 000, 75 wt. % ethylene glycol) were used as received.

3.2. Measurements

^{1}H NMR spectra were recorded on a Bruker Ascend 400 MHz NMR spectrometer in various deuterated solvents (DMSO-d_6, $CDCl_3$ and D_2O). All spectra are shown with normalised intensity of the signal where the solvent signal has been excluded from the normalisation.

SEC measurements were carried out in a Shodex KF-802 GPCH column using Viscotek 250 a dual detector measuring refractive index and viscosity. Chloroform (VWR, HPLC grade) was used as the mobile phase. A polystyrene standard was used for conventional calibration.

Thermogravimetric analysis (TGA) was performed using a TA Instruments Q500 Thermogravimetric Analyzer. In a typical procedure performed under nitrogen flow:

- 1-10 mg sample was added
- The sample was kept at 110 °C for 1 hour.
- Cooled to 50 °C
- Heated to 600 °C at a rate of 10 °C/min measuring weight change

DSC was performed using a TA Instruments Q2000. In a typical procedure:

- The sample (1-10 mg) was put in a closed pan and the pan was put in the instrument cooled to 10 °C, heated to 150 °C 10 °C/min and kept at 150 °C for 10 minutes.
- Measurements started and the sample was cooled to -80 °C, 10 °C/min.
- The sample was heated to 150 °C, 10 °C/min and measurements ended.

[1] Abbreviation (if used), supplier, grade or purity if available

Electrochemical characterisation was limited to conductivity measurements using impedance spectroscopy. The ion conductivity measurements of the electrolytes were performed over a temperature range of 0 to 90 ˚C. Dried electrolyte samples with a diameter of 15 mm and a thickness of 107 µm were sandwiched between two gold-plated brass coin electrodes spaced by a PTFE (polytetrafluoroethylene) ring spacer inside a glove box under argon atmosphere. The measurements were carried out using a computer controlled Novocontrol BDC40 high-resolution dielectric analyzer equipped with a Novocool cryostat unit. Samples were analyzed in the frequency range 10^{-1} - 10^{7} Hz at 50 mV AC amplitude, and the conductivities were subsequently evaluated using the Novocontrol software WinDeta. The plateau value of the conductivity, in the frequency interval at which the conductivity is independent of the frequency, is taken as the conductivity of the sample as shown in Figure 6 below.

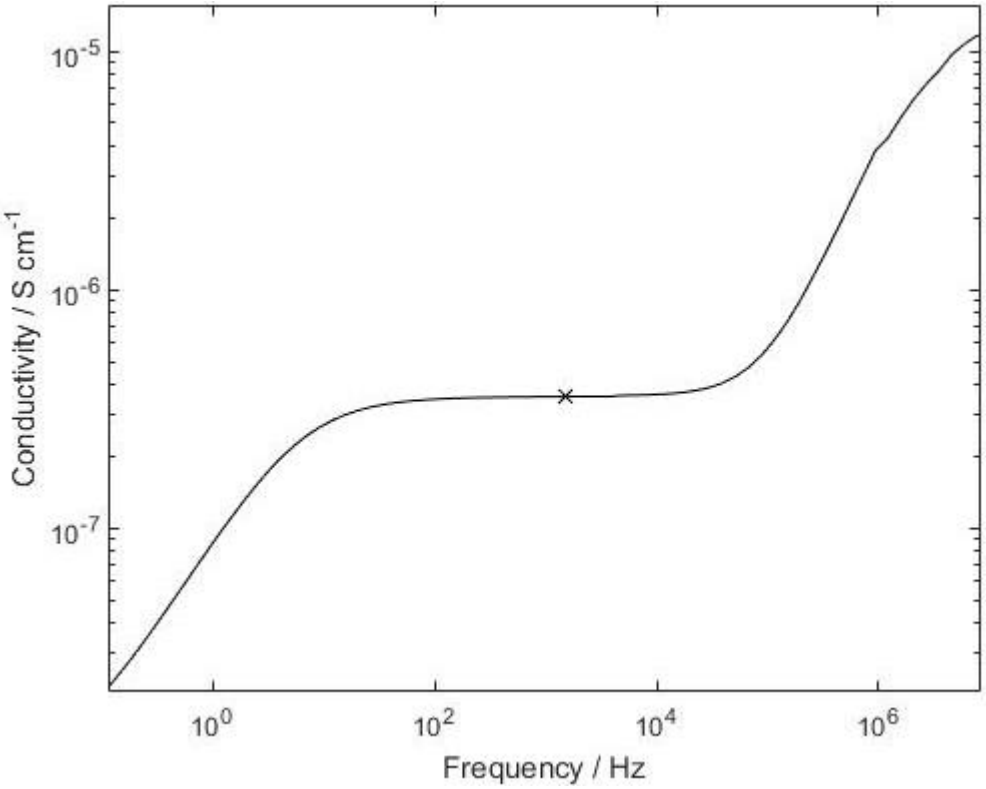

Figure 6. Example of how the conductivity varies with frequency at one temperature, x marks the plateau value that is taken as the conductivity of the sample

3.3. Synthesis

3.3.1. Overall synthesis

Figure 7 below shows the overall synthesis starting from polymerisation of ECH (**1**) to yield PECH (**2**). The synthesised PECH was reacted with triethylene glycol monomethyl ether in different ratio to yield polymer **3-x** with different ratios of y/x, for the homopolymer with y = 0 this reaction was not performed. **3-x** was reacted with 2-methoxyethaneamine to yield **4-x** which was either reacted with sodium 2-bromoethane sulfonate to yield **5-x**, or with 1,4-butanesultone to yield **6-x**. After ion exchange of **5-x** and **6-x** to lithium as counter ion the final product **7-x-i**, with i = 2 and 4 respectively, was obtained.

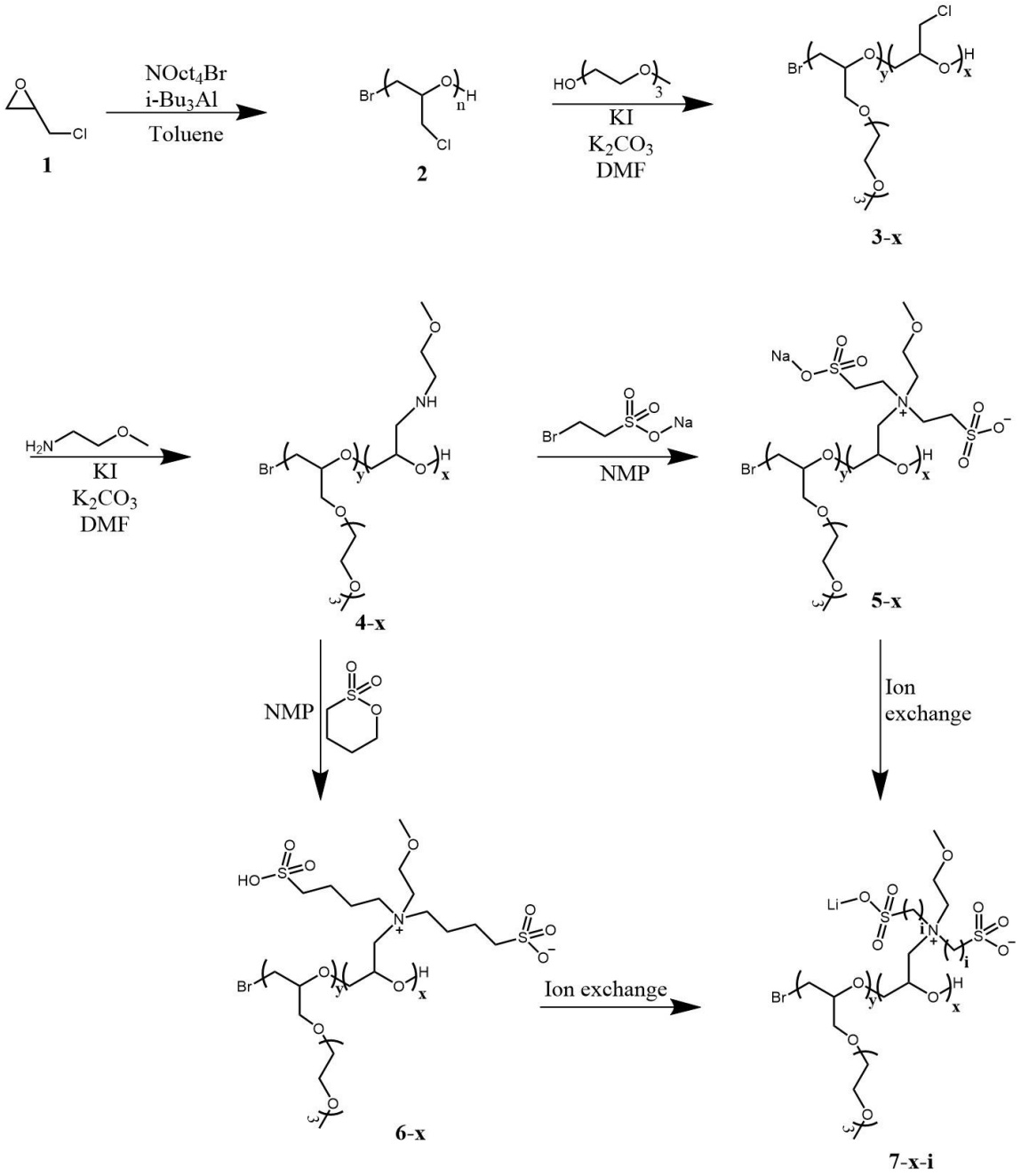

Figure 7. Overall synthesis, x and y denotes molar fractions of the repeating units, i = 2 or 4

3.3.2. Polyepichlorohydrin (PECH) 2

Anhydrous toluene (46 mL), epichlorohydrin (13g, 1 eq.), tetraoctylammonium bromide solution (4.8 ml, 0.003 eq.) and triisobutylaluminium solution (1.04 ml, 0.008 eq.) were mixed under nitrogen at -78 ˚C. The mixture was warmed up slowly to room temperature after 1 hour. A small portion of ethanol (5 mL) was used to quench the polymerization after 16 hours. The solvent was removed under reduced pressure and the product was dried under vacuum at 50 ˚C overnight yielding a product of 11.2 g (86 % yield).

3.3.3. Synthesis and copolymerisation of 2-(2,5,8,11-tetraoxadodec1-yl)-oxirane (EO_3Ox)

2-(2,5,8,11-Tetraoxadodec1-yl)-oxirane was synthesised according to literature [13]. It was attempted to copolymerise EO_3Ox with epichlorohydrin in a similar way as the polymerisation of epichlorohydrin, however this did not work. Heyi Hu have previously used the $Al(i\text{-}Bu)_3/NOct_4Br$ catalytic system for polymerisation of EO_3Ox which yielded polymers with very low molecular weight compared to the value calculated from the monomer to initiator ratio [14]. A cationic ring-opening technique using boron trifluoride diethyl etherate/1,4-butanediol system based on literature [15] was used to copolymerise EO_3Ox and epichlorohydrin however the yield was too low to be useful.

3.3.4. Polymer 3-37

In a typical procedure, PECH (2.05 g, 1 eq.), EO_3Gly (3.6 g, 0.75 eq.), potassium carbonate (4.5 g, 1.13 eq.), potassium iodide (3.6 g, 0.75 eq.) and dimethylformamide (50 mL) were mixed and kept at 100 ˚C for 4 days. After the reaction, dimethylformamide was removed under reduced pressure. The remaining product was dissolved in chloroform, centrifuged and precipitated in hexane twice. The product **3-37** was dried in vacuum at 50 ˚C overnight.

3.3.5. Polymer 4-37

Polymer **3-37** (37 mol % ECH, 4.7 mmol chlorine, 2.16 g, 1 eq.), 2-methoxyethylamine (23.5 mmol, 1.76 g, 5 eq.), potassium carbonate (9.4 mmol, 1.3 g, 2 eq.), potassium iodide (2.4 mmol, 390 mg, 0.5 mmol) and dimethylformamide (50 mL) were mixed and kept at 80 ˚C for 3 days. After the reaction, the solvent was removed under reduced pressure and the crude product was dissolved in chloroform. The undissolved particles were removed by filtration and the solvent of the filtrate was removed under reduced pressure. The concentrated product was dissolved in deionised water and dialysed for 2 days. The product **4-37** was obtained after removal of water and dried under vacuum at 50 ˚C overnight.

3.3.6. Polymer 5-37

Polymer **4-37** (37 mol % amine repeating unit, 1 mmol nitrogen, 0.55 g, 1 eq.) was dissolved in 20 ml NMP. Sodium 2-bromoethanesulfonate (10 mmol, 2.2 g, 10 eq.) was added to the solution. The mixture was stirred at 80 ˚C for seven days, after which it was cooled to room temperature and excess salt was removed by filtration. NMP was evaporated under reduced pressure and the solid residue was purified by dialysis for two days yielding polymer **5-37**.

3.3.7. Polymer 6-37

Polymer **4-37** (37 mol % amine repeating unit, 1 mmol nitrogen, 0.55 g, 1 eq.) was dissolved in 20 ml NMP. 1,4-butanesultone (10 mmol, 1.5 g, 10 eq.) was added to the solution. The mixture was stirred at 80 ˚C for seven days, after which it was cooled to room temperature and excess salt was removed by filtration. NMP was evaporated under reduced pressure and the solid residue was purified by dialysis for two days yielding polymer **6-37**.

3.3.8. Blending with poly(ethylene glycol-ran-propylene glycol) (P[EO-r-PO])

The final polymers **7-x-i** did not form a melt below 140 °C which prevented preparation of samples for impedance spectroscopy. By blending **7-x-i** with P(EO-r-PO) it was plasticised enabling sample preparation. **7-x-i** adds charge carriers to the blends that are primarily dissolved and transported by the P(EO-r-PO).

The homopolymer **7-100-2** was dissolved with P(EO-r-PO) in NMP to yield EO/Li ratio of 4/1, 8/1, 16/1 and 24/1 which are similar to the blends made by Doyle et.al. who blended a polymer containing lithium sulfonate side chains and poly[octa(ethylene glycol) methyl ether methacrylate] [6]. Two blends, with an EO/Li ratio of 16, between P(EO-r-PO) and the copolymers **7-75-2** and **7-50-2** were prepared in NMP. After a homogenous solution was formed, NMP was evaporated at 80 °C under nitrogen. Blends of **7-100-4** (with EO/Li ratios of 8/1, 16/1 and 24/1) were prepared in water since only a limited amount of **7-100-4** could be redissolved in NMP. After a homogenous solution was formed, water was evaporated at 60 °C under nitrogen. The compositions of all the blends **7-x-i-w**, where w denotes the weight percentage **7-x-i**, that were prepared are shown in Table 2 below. The blends were deemed macroscopically homogenous through visual inspection and NMR spectroscopy of several different parts of the blends. Blending using water as solvent was avoided as much as possible due to the fact that in polymer blends, water tends to favour one of the polymers which might cause phase separation and heterogeneous blends when evaporating the solvent. Another reason water was avoided is because the blends should be water free otherwise the conductivity measurements would give an inaccurate value. The blend **7-100-2-25** was prepared in both water and NMP to investigate the solvents effect on conductivity. After evaporation of the solvent, the blends were stored in a glove box under argon atmosphere.

Table 2. Compositions of the prepared blends **7-x-i-w**

Ionic rep. unit / x (mol %)	i	Amount 7-x-i / w (wt. %)	EO/Li ratio
100	2	78	4
100	2	55	8
100	2	35	16
100	2	25	24
75	2	42	16
50	2	58	16
100	4	58	8
100	4	38	16
100	4	28	24

4. Results and discussions

4.1. Synthesis

4.1.1. PECH, 2

The proton NMR spectrum of PECH dissolved in $CDCl_3$ showed a broad band between δ (ppm) 3.75 and 3.59 as previously reported [16]. Molecular weights determined using SEC are shown in Table 3 below. The molecular weight was reasonably high with a low PDI indicating that all chains have roughly the same weight. The theoretical value was determined based on the yield and the molar ratio of the epichlorohydrin monomer and the $NOct_4Br$ initiating species, assuming all chains are activated during the start and keep propagating until the end of the polymerisation. The theoretical value deviates from the molecular weight determined by SEC. This is in part due to the different hydrodynamic volumes of PECH and the standard leading to SEC showing a different value of the molecular weight than what it actually is. The assumptions made when calculating the theoretical value, that all chains are initiated at the same time and grows during the entire polymerisation without termination, is not entirely correct which can also explain the deviation from the theoretical value.

Table 3. Molecular weight of PECH

	M_n (kg/mol)	**M_w (kg/mol)**	**PDI**
SEC measurement	13.2	14.8	1.12
Theoretical	25		

4.1.2. Polymers **3-x**

^{1}H NMR spectra of the polymers **3-x**, synthesised with different ratios of y/x, dissolved in $CDCl_3$ are shown in Figure 8 below. By calculating the ratios between the methyl peaks of **3-x** at 3.37-3.39 and the broad band at 3.8-3.55 (the rest of the hydrogens), the compositions of the polymers were determined to be 37 mol %, 50 mol % and 75 mol % epichlorohydrin repeating unit in the respective polymers. This corresponds to 63, 50 and 25 % substitution of the chloromethyl, in the side chain of PECH, respectively and the goal was to achieve 75, 50 and 25 % substitution. Reaching high degree of substitution is difficult but could be done by using an excess of EO_3Gly. However it would then be difficult to control the amount of substitution. The reaction time would need to be greatly increased to obtain full conversion of EO_3Gly if the aim is to reach a high degree of substitution without using excess EO_3Gly. This is because of the low concentration of the chloromethyl once the substitution reaches a sufficiently high value.

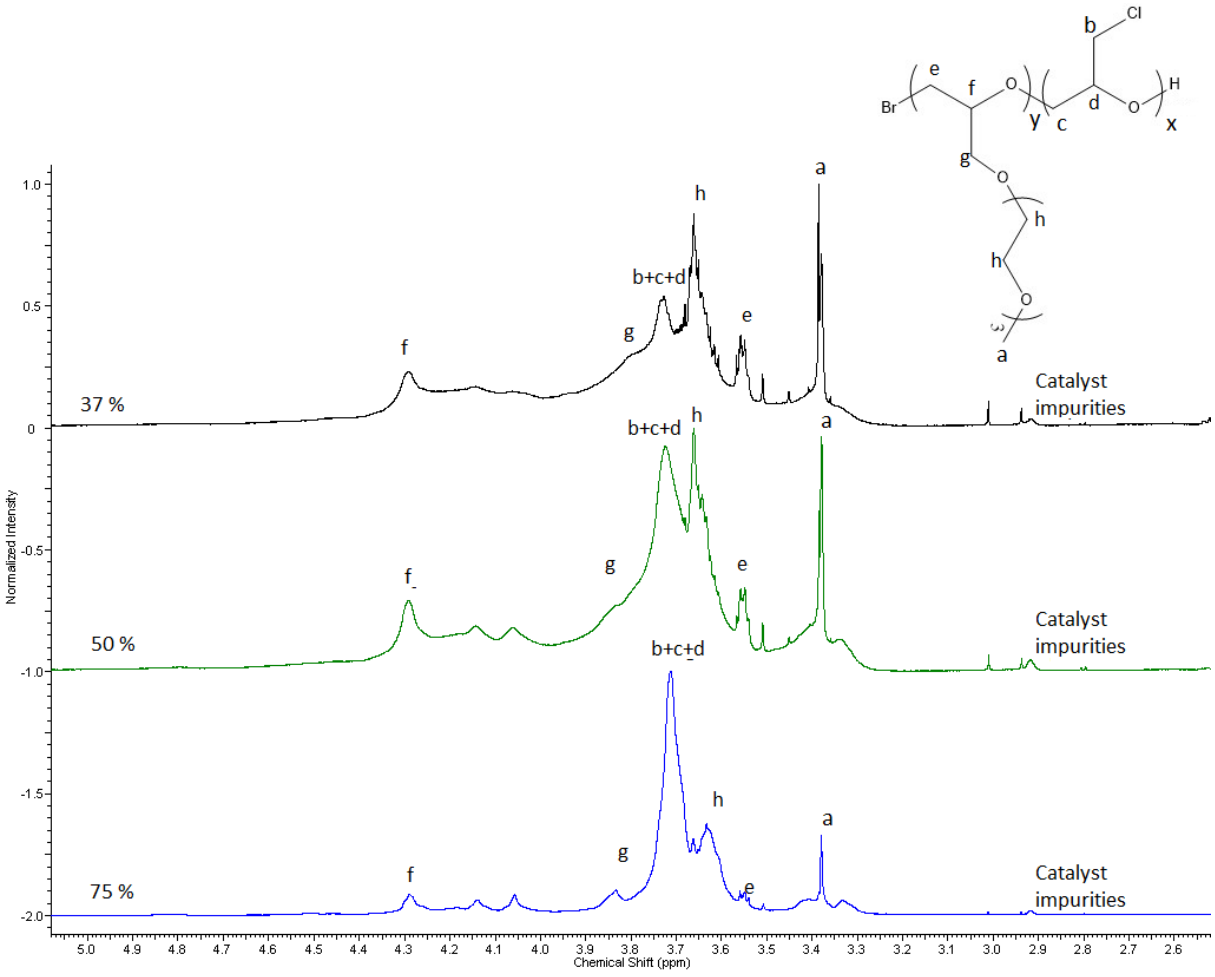

Figure 8. ^{1}H NMR spectra of polymer **3-x** in $CDCl_3$. Black 37 mol % ECH, green 50 mol % and blue 75 mol %. Distinct peaks marked in the figure and the broad peaks are caused by all the other hydrogen in the molecule. Catalyst impurities from polymerisation present at 2.9 ppm

4.1.3. Polymers **4-x**

^{1}H NMR spectra of the polymers **4-x** are shown in Figure 9 below. The signal b of the hydrogen bonded to the nitrogen are in the correct ratios compared to the broad beaks above 3.3 ppm for full substitution of the chloromethyl.

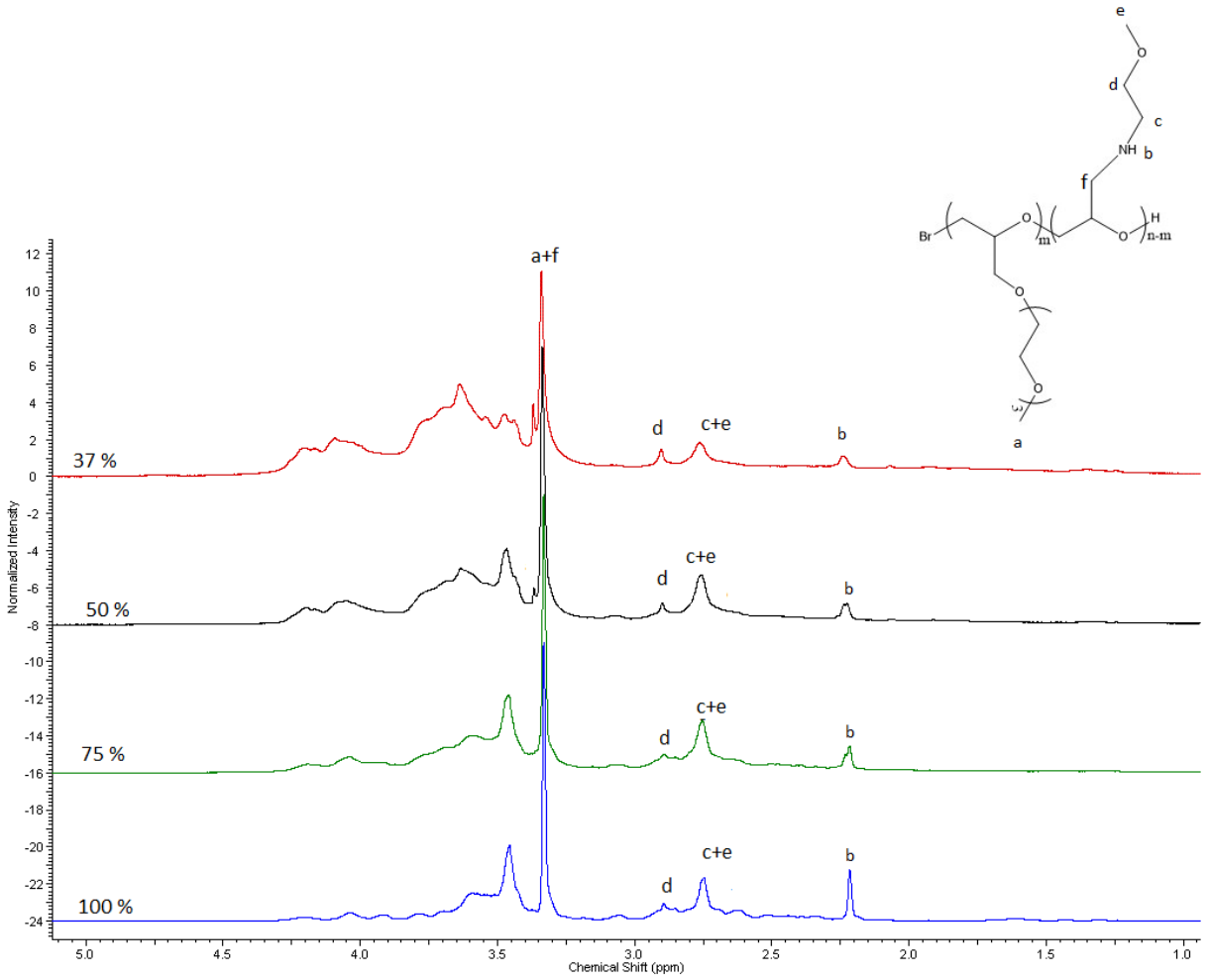

Figure 9. ^{1}H NMR spectra of **4** in $CDCl_3$, Red 37 mol % repeating unit with amine, black 50 mol %, green 75 mol % and blue 100 %. Distinct peaks marked in the figure. The broad peaks are caused by all the other hydrogen in the molecule

4.1.4. Polymers **7-x-i**

^{1}H NMR spectra of **7-x-i** are shown in Figure 10 and Figure 11. By studying and comparing the spectra with each other and the reactants used in the quarterisation, some of the more distinct peaks were identified. The letters shown in Figure 10 and Figure 11 correspond to hydrogens bonded to atoms marked with the same letter. The degree of polymerisation of the synthesised PECH, the molecular weight of the repeating units and the compositions of **7-x-i** were used to calculate the final molecular weights of the polymers that are shown in Table 4.

Table 4. Composition, EO/Li ratio and molecular weight of **7-x-i**

i	**Ionic repeating unit (mol %)**	**Ionic repeating unit (wt. %)**	**EO/Li (mol ratio)**	M_n **(kg mol^{-1})**
2	37	49	11/1	38
2	50	62	7/1	41
2	75	83	3,7/1	46
2	100	100	2/1	50
4	37	52	11/1	41
4	50	65	7/1	45
4	75	85	3,7/1	52
4	100	100	2/1	58

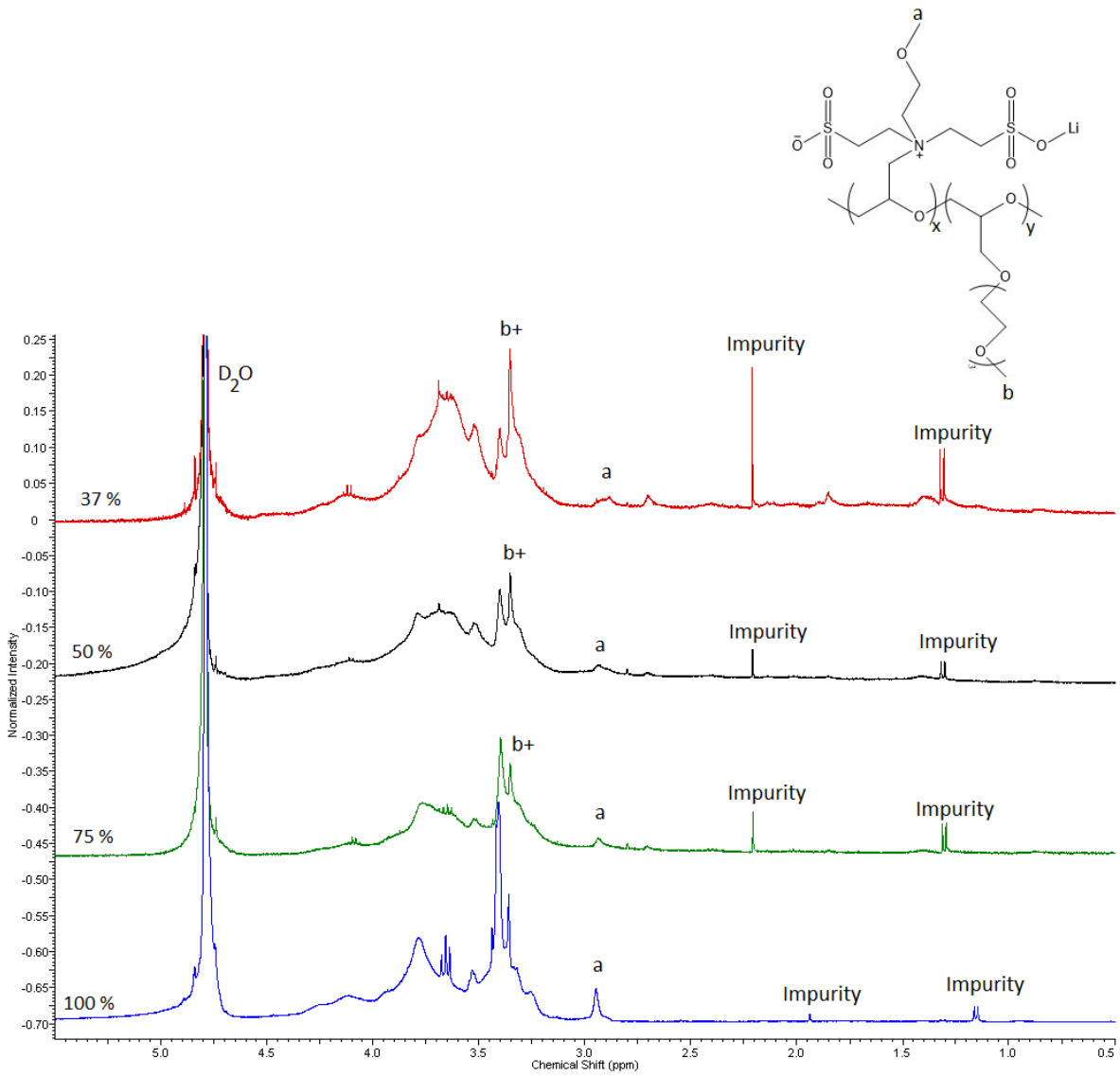

Figure 10. ^{1}H NMR spectra of **7-x-2** in D_2O, Red 37 mol % ionic repeating unit, black 50 mol %, green 75 mol % and blue 100 mol %. Impurity also present in blank of D_2O. Peak b is from hydrogen at b as well as other hydrogen at polymer

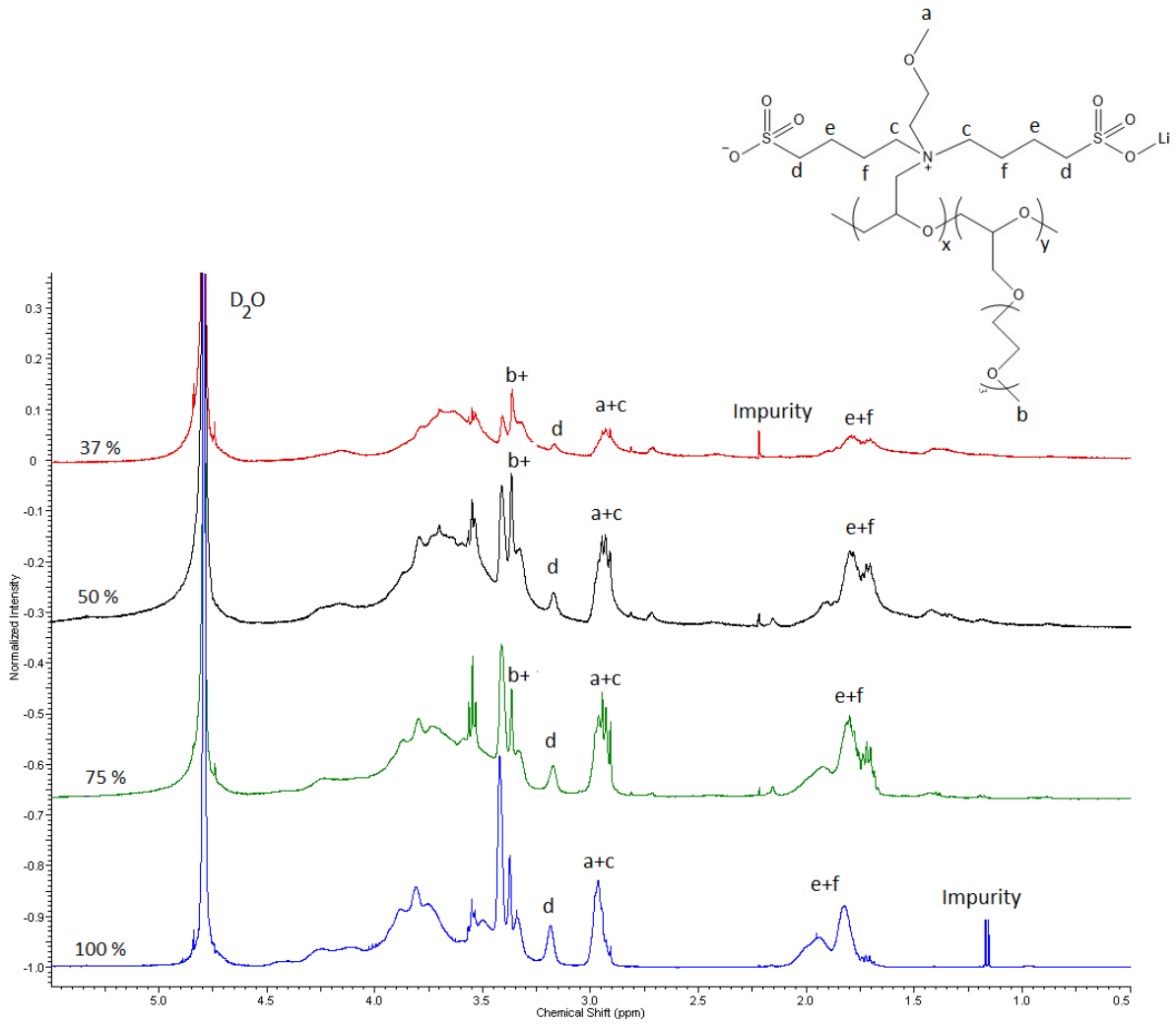

Figure 11. ^{1}H NMR spectra of **7-x-4** in D_2O, Red 37 mol % ionic repeating unit, black 50 mol %, green 75 mol % and blue 100 mol %. Impurity also present in blank of D_2O. Peak b is from hydrogen at b as well as other hydrogen at polymer

4.2. TGA

TGA curves for the polymers **7-x-i** are shown in Figure 12 and their degradation temperatures, defined here as the temperature at which the weight is 95 % of its original value, are shown in Table 5 below. All polymers were stable up to 240 °C which is sufficient for use in LIBs. **7-x-2** degraded at lower temperatures compared to **7-x-4**. For **7-x-2** all the polymers had similar degradation temperatures of roughly 240 °C and at 600 °C there was a trend that the polymers with higher content of ionic repeating unit had less ash content. **7-37-4** degraded at 240 °C, **7-x-4** with higher content of the ionic part degraded at around 250 °C and there was a trend in the degree of degradation decreased with increasing ionic content. The ash content of **7-100-4** was less than for the copolymers but there was no clear trend in the ash content in the copolymers **7-x-4**. It might be that parts of the non-ionic side degraded first at around 220°C and then at slightly higher temperatures parts of the ionic repeating unit started to degrade.

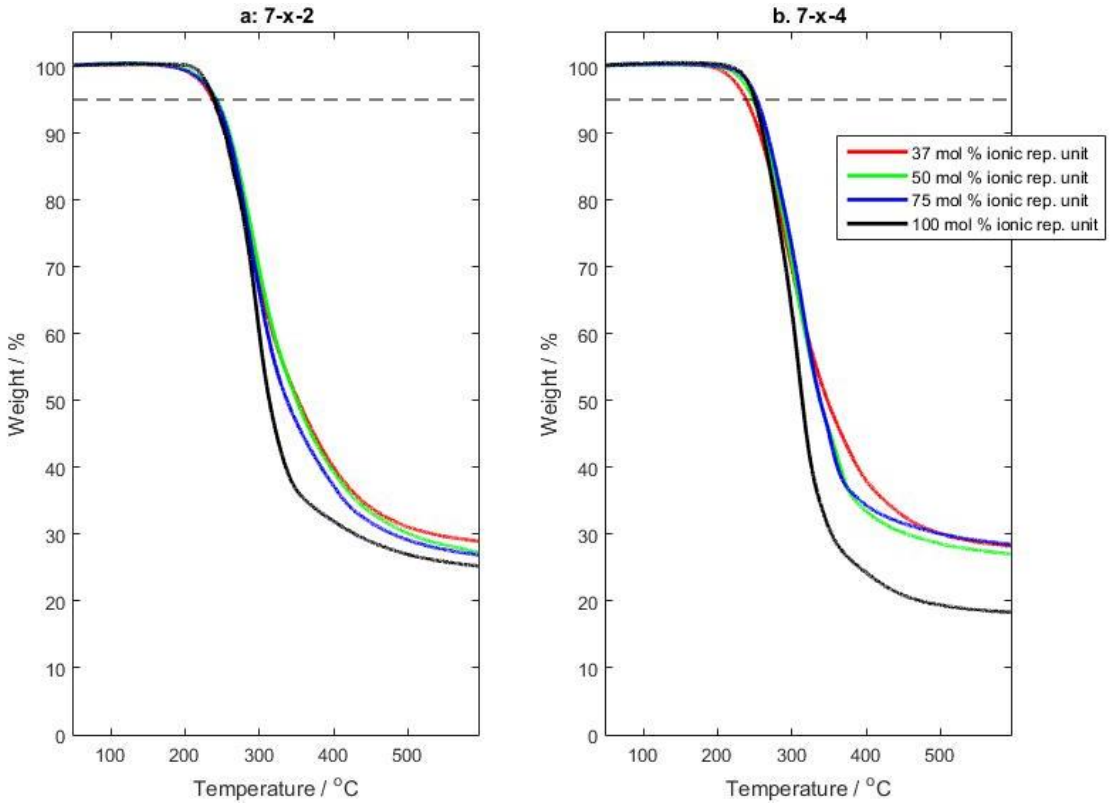

Figure 12. TGA curve of **a: 7-x-2** and **b: 7-x-4**, dashed line show 95 wt. %

Table 5. Degradation temperature of **7-x-i**

	37 mol % ionic rep. unit	**50 mol % ionic rep. unit**	**75 mol % ionic rep. unit**	**100 mol % ionic rep. unit**
i = 2	238 °C	243 °C	241 °C	240 °C
i = 4	239 °C	248 °C	250 °C	250 °C

4.3. DSC

The DSC curves of **7-x-2** and **7-x-4** are shown in Figure 13 and Figure 14 below and the glass transition temperatures for the polymers are shown in Table 6 below. The polymers **7-x-2** had a lower glass transition temperature compared to **7-x-4** and increasing the amount of ionic content increased the T_g, as shown in Figure 15. In some part this can be explained by the increase in molecular weight of the **7-x-i** with high content of ionic repeating unit, because the higher molecular weight of the ionic repeating unit, increased the T_g. The polymers had sufficiently high molecular weights that this effect only showed minor contribution to the difference in T_g. The primary reason for increased T_g was that the ionic repeating units gave a higher T_g than the non-ionic. The T_g for a polymer with 0 % ionic repeating unit and a molecular weight of 3.4 kg mol^{-1} has previously been measured to be -52 °C [15].

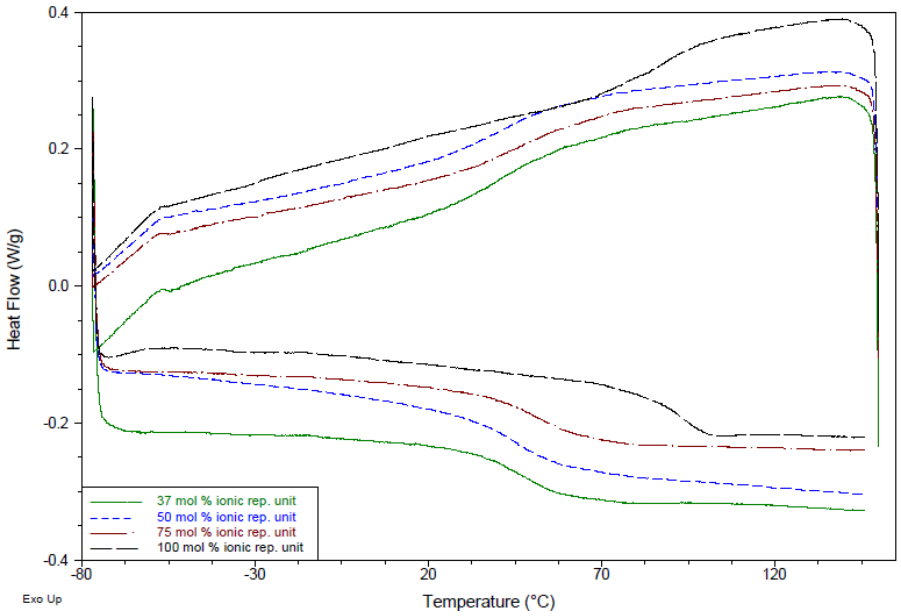

Figure 13. DSC curve of **7-x-2** from -80 °C to 150 °C

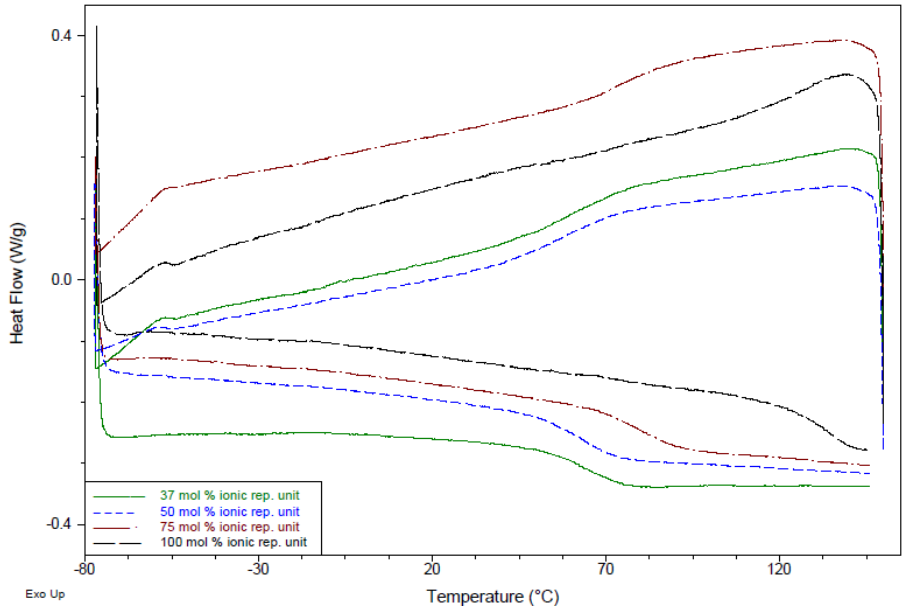

Figure 14. DSC curve of **7-x-4** from -80 °C to 150 °C

Table 6. Glass transition temperatures of **7-x-i**

	37 mol % ionic rep. unit	**50 mol % ionic rep. unit**	**75 mol % ionic rep. unit**	**100 mol % ionic rep. unit**
i = 2	42 °C	46 °C	57 °C	95 °C
i = 4	62 °C	64 °C	80 °C	132 °C

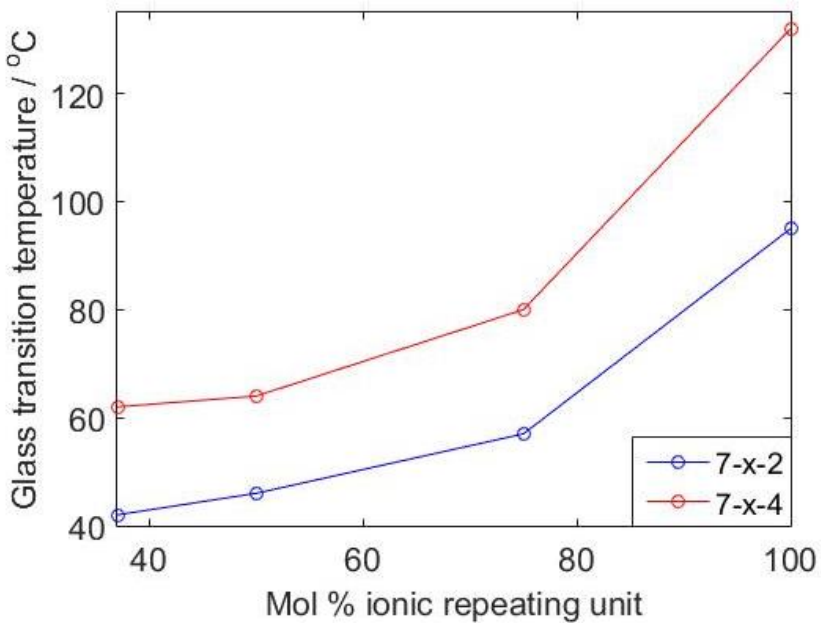

Figure 15. T_g of **7-x-i** as a function of the amount of ionic repeating unit. Higher content of ionic repeating unit increases T_g

The DSC curves of the homopolymers **7-100-2** and **7-100-4** blended with P(EO-r-PO) are shown in Figure 16 and Figure 17. All the blends had T_gs around -65 °C regardless of the amount of **7-x-i**. There was a second T_g around -30 °C which would indicate that the blends were not entirely homogenous. The results from the DSC indicate that the polymers were not molecularly miscible, phase separation occurred and the blends were microscopically heterogeneous. In the blends there was a likely presence of a pure phase of P(EO-r-PO) with a T_g of -65 °C and another phase that was a homogenous mixture of **7-x-i** and P(EO-r-PO) where the T_g of **7-x-i** had been greatly decreased to around -30 °C. The addition of **7-x-i** increased the crystallisation temperature, it could be that **7-x-i** facilitated in the crystallisation of P(EO-r-PO) by acting as nucleating sites during the crystallisation. The fact that crystallisation took place in the blends also indicates that the polymers were not molecularly miscible and the blends were microscopically heterogeneous.

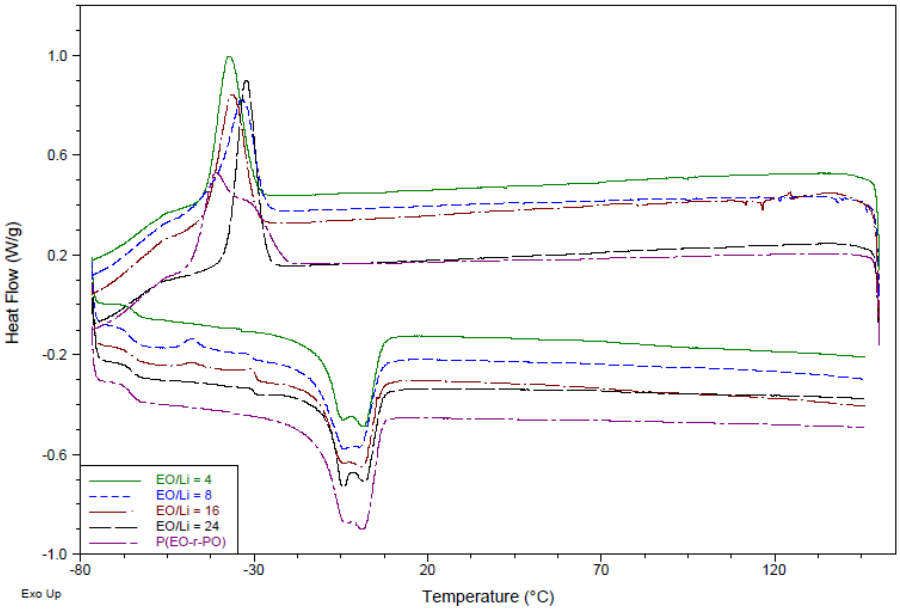

Figure 16. DSC curves of blends between **7-x-2** and P(EO-r-PO) from -80 °C to 150 °C

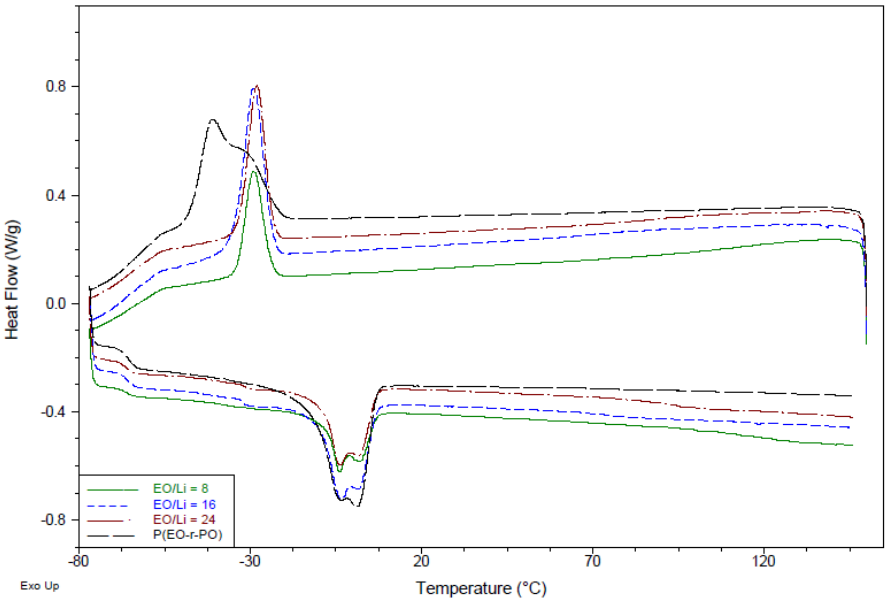

Figure 17. DSC curves of blends between **7-x-4** and P(EO-r-PO) from -80 °C to 150 °C

The DSC curves of the copolymer blends with EO/Li ratio of 16 are shown in Figure 18. None of the copolymers were molecularly miscible with the P(EO-r-PO) and glass transition and melting temperatures of the blends were similar to the previous blends. The blends had T_g at -65 °C, a second T_g at -30 °C and melting points at around 0 °C.

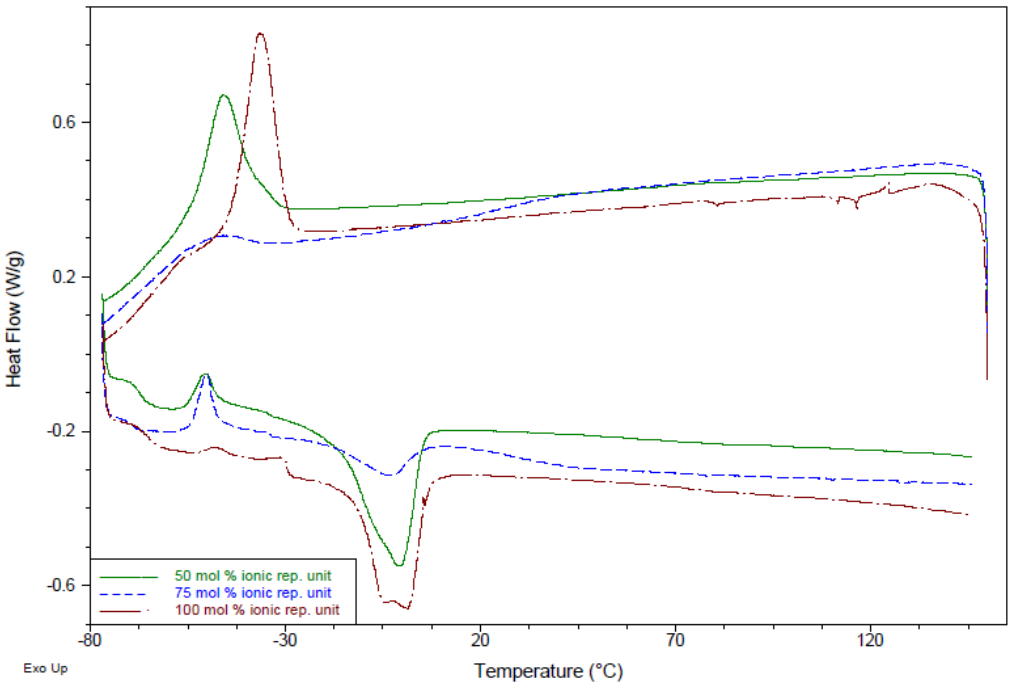

Figure 18. DSC curves of blends between **7-x-2** and P(EO-r-PO) with EO/Li = 16 from -80 °C to 150 °C

4.4. Conductivity

How the conductivity varies, at different temperatures, for the blend **7-100-2-25** prepared using both water and NMP as solvent is shown in Figure 19 below. The solvent used during the blending had no effect on the conductivity and it is possible to compare the blends **7-x-i-w** even if they were not prepared using the same solvents.

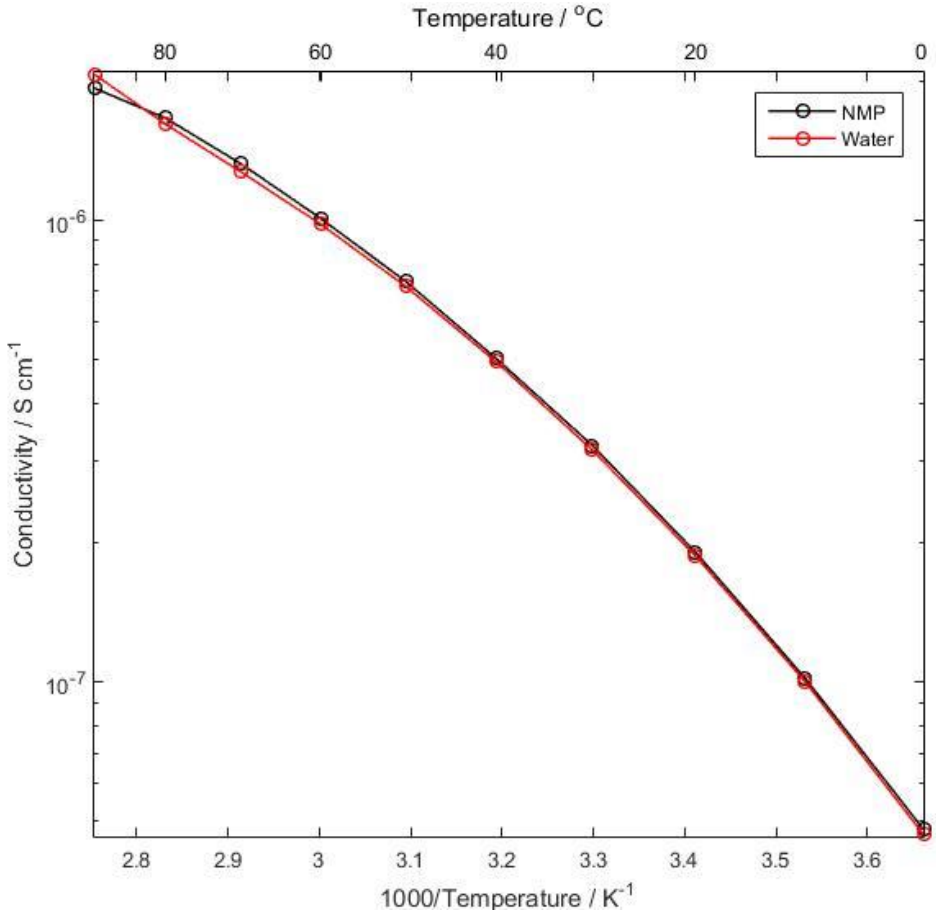

Figure 19. Conductivity of the blend **7-100-2-25** (EO/Li = 24) prepared in NMP and water. The solvent used in the blending had no effect on the conductivity.

Figure 20 shows the conductivity of the blends **7-100-i-w** from 0°C to 90 °C and the maximum conductivity, at 90 °C, is also shown in Table 7. Since the amount of **7-100-i** in the blends only had a small effect on the melting and glass transition temperatures, increase of the charge carrier concentration (lower EO/Li ratio) increased the conductivity in the blends **7-100-2-w** to a maximum of $3.3 \cdot 10^{-6}$ S/cm at an EO/Li ratio of 8 (corresponding to the blend **7-100-2-55**) at 90 °C. Further decrease of the EO/Li ratio lead to a decrease in conductivity. This might have been because the ethylene oxide units were unable to participate in more coordination complexes and solvate more lithium ions at lower EO/Li ratios. In the blends **7-100-4-w** the conductivity was around $2 \cdot 10^{-7}$ S/cm for the high EO/Li ratios. It then decreased tenfold. This might have been because P(EO-r-PO) failed to solvate the Li^+ ions in these blends to the same degree as in **7-100-2-w**. When the amount of P(EO-r-PO) was decreased even less Li^+ was solvated resulting in less dissolved charge carriers and lower conductivity. The conductivities were similar to the conductivities of other single-ion conductors however they were too low for the blends to be of direct use as electrolytes in LIBs. It might be that sulfonate groups can coordinate and capture lithium ions, as illustrated in Figure 21a-b, explaining the low conductivity of **7-100-i-w.** The tenfold reduction of conductivity between **7-100-2-w** and **7-100-4-w**, might be explained by the increased length and flexibility of the carbon chains of the sulfonate groups facilitates ion capture and hence lowers the conductivity. Making the carbon chains of the sulfonate groups more rigidly bonded to the polymer, as shown in Figure 21c, might inhibit capture and increase the conductivity.

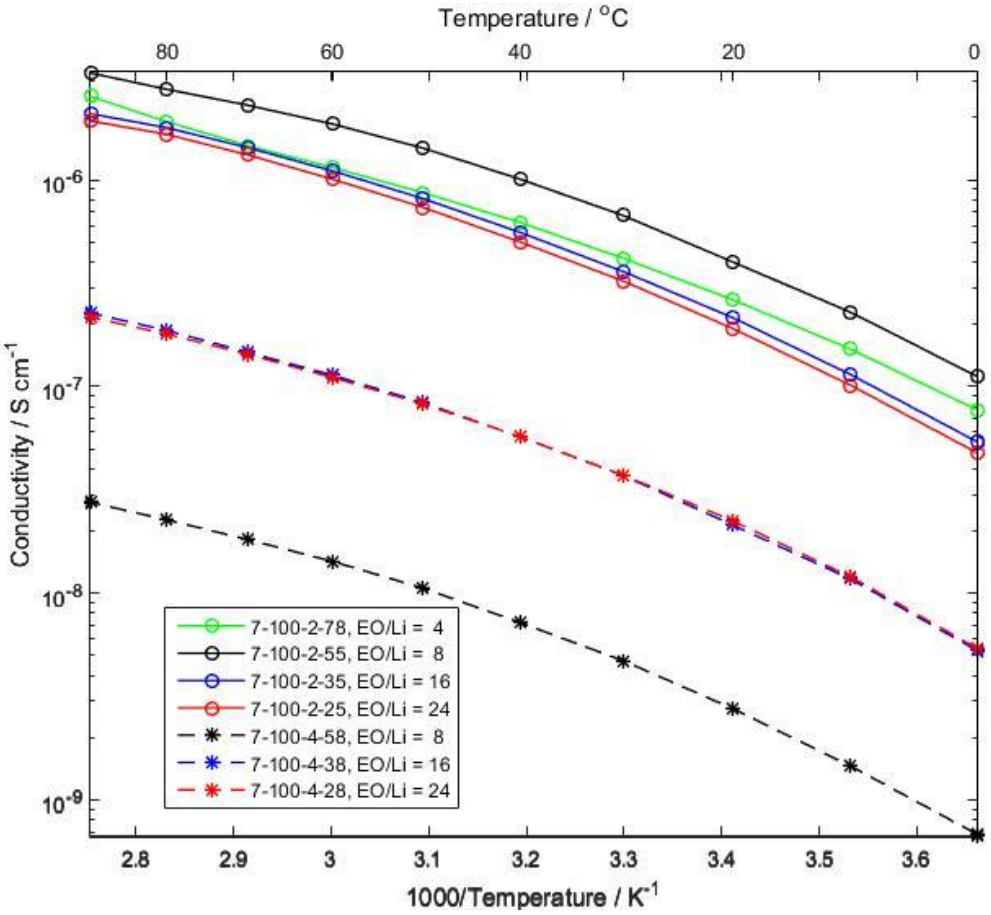

Figure 20. Conductivity of the blends **7-100-i-w** between 0 °C and 90 °C

Table 7. Conductivity (in 10^{-6} S/cm) of the blends **7-100-i-w** at 90 °C

	EO/Li = 4	**EO/Li = 8**	**EO/Li = 16**	**EO/Li = 24**
7-100-2-w	2.5	3.3	2.1	1.9
7-100-4-w	-	0.028	0.23	0.22

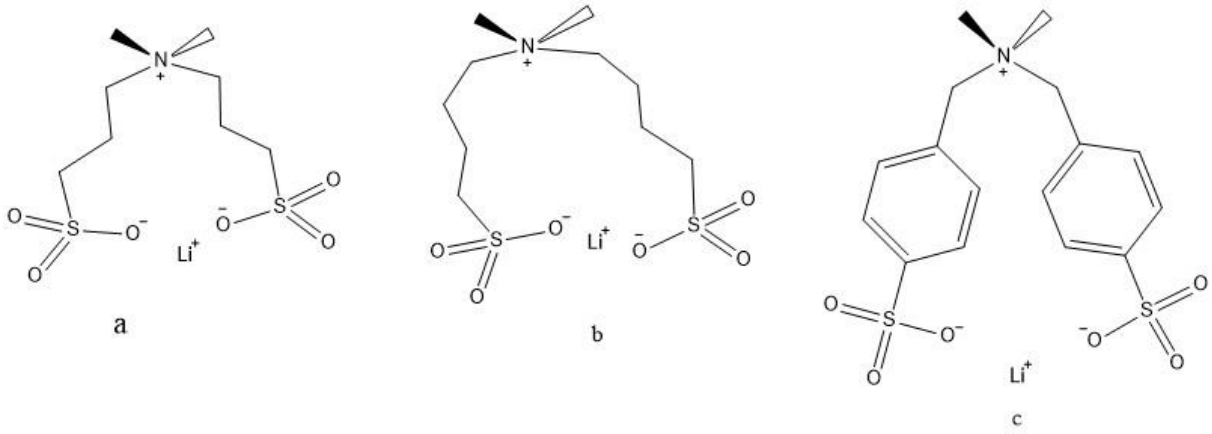

Figure 21a. Coordination between a lithium cation and the ionic side chain of **7-x-2 b.** The coordination between Li^+ and the more flexible side chain of **7-x-4** might be less strained and easier to form **c.** A rigid ionic side chain could possibly only form loose coordination with Li^+.

The conductivity, as a function of temperature, of the copolymer blends **7-x-2-w** with an EO/Li ratio of 16 is shown in Figure 22 below. Copolymers with low content of ionic repeating unit were blended with less P(EO-r-PO), to yield the same EO/Li ratio as a copolymer with high content of ionic repeating unit. A copolymer with low content of ionic repeating unit was plasticised less in the blend and the conductivity was lower compared to the blend **7-100-2-35**. It might be that a copolymer that has not been blended would have a lower conductivity than a blend with the same EO/Li ratio, due to the plasticising effect of the P(EO-r-PO).

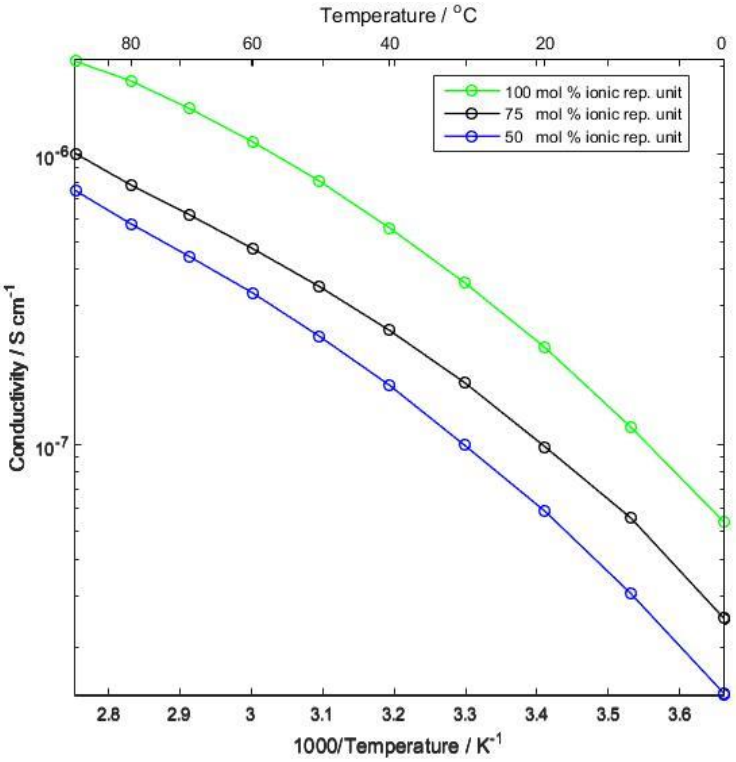

Figure 22. Conductivity of blends **7-x-2-w** with EO/Li = 16 between 0 °C and 90 °C. The molar fractions ionic repeating unit, **x,** of the respective polymer **7-x-2** are shown in the figure.

5. Conclusion

A synthetic pathway to the target copolymers has been developed by polymerisation of epichlorohydrin followed by several post-polymerisation reactions. The synthesised polymers were thermally stable but had high glass transition temperatures that likely preclude them from electrolyte applications. They did not form a melt at sufficiently low temperatures for preparation of samples for conductivity measurements and might have a low conductivity due to the high glass transition temperatures. The blends between **7-100-i** and P(EO-r-PO) prepared had conductivities that were similar to other single-ion conductors and were too low for direct use in electrolyte applications. The blends **7-100-2-w** had generally a higher conductivity than the blends **7-100-4-w**, which might have been due to the increased flexibility of the sulfonate groups in **7-100-4** which could facilitate ion capture. The maximum conductivity measured was $3.3 \cdot 10^{-6}$ S/cm at 90° for the blend **7-100-2-55** (EO/Li ratio of 8). The conductivities of the blends of the copolymers might indicate that blending **7-x-i** results in a higher conductivity than using a copolymer with the same EO/Li ratio.

6. Future work

One suggestion is to synthesise copolymers with lower ionic content and higher EO/Li ratio to further lower the glass transition that the copolymers can be melted at sufficiently low temperatures for electrolyte preparation and conductivity. However this might result in electrolytes with an ionic conductivity lower than that of the blends prepared. Another idea is to synthesise polymer in which the sulfonate groups are more rigid to prevent them from coordinating and capturing lithium ions in the electrolyte. An additional suggestion is to plasticise **7-x-i** with a low molecular weight solvent, that can be completely absorbed by the polymer, to measure the conductivity of the plasticised polymer in a homogenous system.

7. Refrences

[1] Z. Xue, D. He and X. Xie, “Poly(ethylene oxide)-based electrolytes for lithium-ion batteries,” *J. Mater. Chem A,* vol. 3, pp. 19218-19253, 2015.

[2] D. T. Hallinan and N. P. Balsara, “Polymer Electrolytes,” *Annu. Rev. Mater. Res,* vol. 43, pp. 503-525, 2013.

[3] D. E. Fenton, J. M. Parker and P. V. Wright, “Complexes of alkali-metal ions with poly(ethylene oxide),” *Polymer,* vol. 14, p. 589, 1973.

[4] L. E. Smart och E. A. Moore, Solid State Chemistry: An Introduction, Boca Raton: CRC Press, 2012, pp. 226-227.

[5] J. B. Goodenough and K.-S. Park, “The Li-Ion Rechargeable Battery: A perspective,” *J. Am. Chem. Soc,* vol. 135, no. 4, pp. 1167-1176, 2013.

[6] R. P. Doyle, X. Chen, M. Macrae, A. Srungavarapu, L. J. Smith, M. Gopinadhan, C. O. Osuji och S. Granados-Focil, ”Poly(ethylenimine)-Based Polymer Blends as Single-Ion Lithium Conductors,” *Macromolecules,* vol. 14, pp. 3401-3408, 2014.

[7] D. Mecerreyes, ”Polymeric ionic liquids: Broadening the properties and applications of polyelectrolytes,” *Prog. Polym. Sci.,* vol. 36, nr 12, pp. 1629-1648, 2011.

[8] S. Feng, D. Shi, F. Liu, Z. Liping, N. Jin, W. Feng, X. Huang, M. Armand och Z. Zhou, ”Single lithium-ion conducting polymer electrolytes based on poly[(4-styrenesulfonyl)(trifluoromethanesulfonyl)imide] anions,” *Electrochim Acta,* vol. 93, pp. 254-263, 2013.

[9] S. Carlotti, A. Labbé, V. Rejsek, S. Doutaz, M. Gervais och A. Deffieux, ”Living/Controlled Anionic Polymerization and Copolymerization of Epichlorhydrin with Tetraoctylammonium Bromide-Triisobutlyaluminum Initiating Systems,” *Macromolecules,* vol. 41, pp. 7058-7062, 2008.

[10] J. M. G. Cowie och V. Arrighi, Polymers: chemistry and physics of modern materials, III red., Boca Raton: CRC Press, 2007, pp. 243-245.

[11] J. R. Fried, Polymer Science and Technology, 2 ed., Upper Saddle River: Prentice Hall Professional Technical Reference, 2007, pp. 174-175.

[12] A. Lasia, Electrochemical Impedance Spectroscopy and its Applications, New York: Plenum Publishers, 1999, pp. 4-7.

[13] Y. Liu, Y. Wang, W. Yufeng, J. Lu, V. Piñón och M. Weck, ”Supporting Information of Shell Cross-linked Micelle-Based Nanoreactors for the Substrate-Selective Hydrolytic Kinetic Resolution of Epoxides,” *J. Am. Chem. Soc,* vol. 133, nr 36, pp. S-16, 2011.

[14] H. Hu, ”Synthesis of poly(ionic liquids) both in solution and on surface of silica nanoparticles as novel quasi-solid state electrolytes,” Michigan State University, East Lansing, 2013.

[15] H. Hu, W. Yuan, Z. Jia och G. L. Baker, ”Ionic liquid-based random copolymers: a new type of polymer electrolyte with low glass transition temperature,” *RSC Adv.,* vol. 5, pp. 3135-3140, 2015.

[16] C. He, C. Zhang, M. Xi och S. Zhang, ”Synthesis and characterization of polyepichlorohydrin-based copolymers with biphenyl groups attached thioether unit,” *J. Wuhan. Univ. Technol.,* vol. 25, nr 3, pp. 487-491, 2010.

8. List of figures

9. List of tables